

---

# Confidence Calibration with Bounded Error Using Transformations

---

Sooyong Jang<sup>1</sup> Radoslav Ivanov<sup>1</sup> Insup Lee<sup>1</sup> James Weimer<sup>1</sup>

## Abstract

As machine learning techniques become widely adopted in new domains, especially in safety-critical systems such as autonomous vehicles, it is crucial to provide accurate output uncertainty estimation. As a result, many approaches have been proposed to calibrate neural networks to accurately estimate the likelihood of misclassification. However, while these methods achieve low expected calibration error (ECE), few techniques provide theoretical performance guarantees on the calibration error (CE). In this paper, we introduce Hoki, a novel calibration algorithm with a theoretical bound on the CE. Hoki works by transforming the neural network logits and/or inputs and recursively performing calibration leveraging the information from the corresponding change in the output. We provide a PAC-like bounds on CE that is shown to decrease with the number of samples used for calibration, and increase proportionally with ECE and the number of discrete bins used to calculate ECE. We perform experiments on multiple datasets, including ImageNet, and show that the proposed approach generally outperforms state-of-the-art calibration algorithms across multiple datasets and models – providing nearly an order or magnitude improvement in ECE on ImageNet. In addition, Hoki is fast algorithm which is comparable to temperature scaling in terms of learning time.

## 1. Introduction

Deep neural networks have proven useful in various fields such as image classification (He et al., 2016; Zagoruyko & Komodakis, 2016; Tan & Le, 2019), object detection (Redmon & Farhadi, 2018; Bochkovskiy et al., 2020), and speaker verification (Li et al., 2017). Motivated by these successes, deep neural networks have begun to be integrated into safety-critical systems such as medical systems (Ronneberger et al., 2015; Arcadu et al., 2019). However, as observed by Guo et al. (2017), neural networks are often over-confident on their predictions. This over-confidence can be a critical problem in the

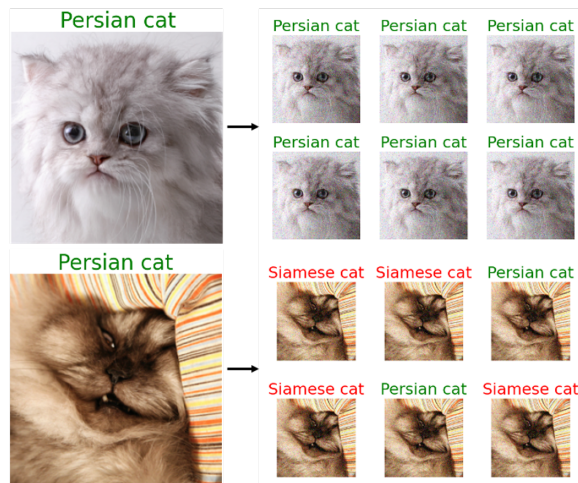


Figure 1. Label predictions can change after image transformations in some images. Here we apply six different Gaussian noise  $N(0, 0.16^2)$  to both original images. Our Intuition: the image with fewer prediction changes should have higher confidence.

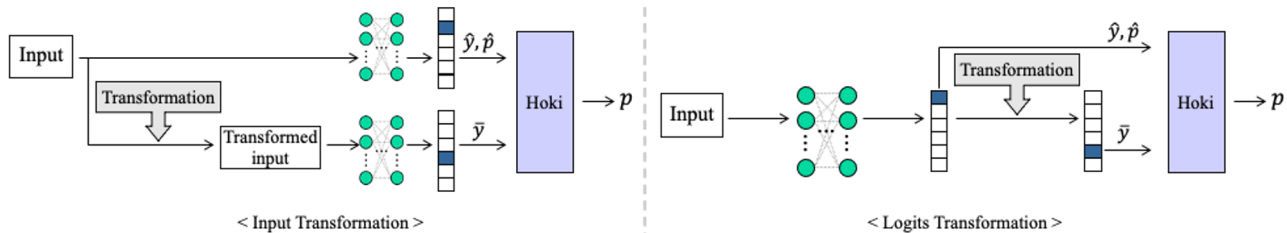


Figure 2. Proposed calibration method. We can use input transformation (left) and/or logits transformation (right). The original prediction and confidence with the prediction for the transformed input (logits) will be used for our calibration. Logits transformation also can be applied after the input transformation.

safety-critical applications where over-confident neural networks can be wrong with high confidence.

Due to the miscalibration of the recent neural networks classifiers, various calibration techniques have been proposed. A common approach is to map uncalibrated logits or confidences to calibrated ones (Guo et al., 2017; Gupta et al., 2020; Jang et al., 2020; Patel et al., 2020; Platt et al., 1999; Kull et al., 2019; Rahimi et al., 2020; Wenger et al., 2020). Another option is to train a neural network with a modified loss function to produce calibrated confidence (Tran et al., 2019; Kumar et al., 2018; Seo et al., 2019). Although existing methods successfully improve the confidence in terms of calibration metrics such as the expected calibration error (ECE) (Naeini et al., 2015), few techniques provide theoretical guarantees on their performance, which is critical if such approaches are used in safety-critical applications.

In response to the need for a theoretical error bound, a few approaches (Kumar et al., 2019; Park et al., 2020) have been proposed to provide theoretical error guarantees on an individual example or on the entire dataset. Kumar et al. (2019) introduce a scaling-binning calibrator based on Platt scaling and histogram binning. Although they provide a bound on the  $\ell_2$  calibration error, they do not provide a bound on the debiased estimator of ECE. Park et al. (2020) propose a method to compute confidence with a bound on individual examples using Clopper-Pearson confidence interval and binning. Although their algorithm can be used for fast DNN inference and safe planning, it assigns the same bound to examples in the same bin.

In this work, we propose Hoki, a calibration algorithm with theoretical performance guarantees (in terms of ECE) that also achieves strong empirical performance as compared with state-of-the-art techniques. The intuition behind Hoki is illustrated in Figure 1. Suppose we are given two images of Persian cats that are initially correctly classified and suppose that we randomly perturb each image a number of times. If all perturbed versions of the first image are still correctly classified whereas the second image transformations lead to label switches (e.g., to Siamese cat), then intuitively we would assign a higher confidence score to the first image’s label. More generally, the idea, as illustrated in Figure 2, is to use such input/logit transformations to test the network’s sensitivity and group examples according to the proportion of observed label switches.

Based on this intuition, we first present sufficient conditions for perfect calibration in terms of ECE through leveraging the information from changes after transformations. Furthermore, since this sufficient condition only holds in expectation, we also provide a bound on the generalization calibration error, given a training dataset. An added benefit of these results is that they also lead to a natural implementation, through minimizing the empirical calibration error (including transformations). The proposed algorithm is also efficient in terms of runtime, especially in the case of logit transformations due to their reduced dimensionality (as compared to the input space dimensionality).

To evaluate Hoki, we perform experiments on MNIST, CIFAR10/100, and ImageNet, and we use several standard models per dataset, including LeNet5, DesneNet, ResNet, and ResNet SD. On these datasets, we compare Hoki with several state-of-the-art calibration algorithms, namely temperature scaling (Guo et al., 2017), MS-ODIR, Dir-ODIR (Kull et al., 2019), and ReCal (Jang et al., 2020). In terms of ECE (Naeini et al., 2015), Hoki outperforms other calibration algorithms on 10 out of 15 benchmarks; we emphasize that Hoki achieves an order of magnitude lower ECE than other methods on all ImageNet models. Finally, in terms of learning time, Hoki achieves similar performance to temperature scaling, the fastest algorithm we compared with.

The main contributions of this paper are as follows:

- We propose Hoki, an iterative calibration algorithm using logits and/or inputs transformations.
- We provide a sufficient condition for perfect calibration and a generalization bound on calibration error.
- We show that Hoki outperforms other calibration algorithms on 10 out of 15 benchmarks, and achieves the lowest ECE on all ImageNet models.
- We demonstrate that Hoki is also efficient in terms of learning time, achieving performance comparable to temperature scaling.

This paper is structured as follows. In Section 2, we summarize the related works, and in Section 3, we describe the problem statement. Then, we present a theory calibration through transformations in Section 4. In Section 5, we demonstrate how a transformation can be selected, and we illustrate the calibration algorithm using transformations in Section 6. In Section 7, we show the experimental results, and we conclude this paper in Section 8.

## 2. Related work

Various approaches have been tried for obtaining accurate confidences, and in this paper, we consider the papers related to our approaches. Our approach is a post-hoc calibration which uses a validation set to calibrate confidences. It also employs a transformation for the calibration, and provides a bound on calibration error. We review post-hoc calibration techniques, transformation based calibration, and also calibration with a theoretical guarantee.

**Post-hoc Calibration.** Many researchers have proposed calibration methods for a neural network classifier so that the predicted probabilities match the empirical probabilities using a validation set (Gupta et al., 2020; Patel et al., 2020; Platt et al., 1999; Guo et al., 2017; Kull et al., 2019; Rahimi et al., 2020; Tran et al., 2019). They scale uncalibrated logits (or confidences) to obtain calibrated values, for example, Platt scaling (Platt et al., 1999), temperature scaling, vector scaling (Guo et al., 2017), or learn a function for the mapping from uncalibrated values to calibrated values (Gupta et al., 2020; Patel et al., 2020; Kull et al., 2019; Rahimi et al., 2020). These approaches, however, do not provide theoretical guarantee on the performance.

**Transformation-based calibration.** Another approach using input transformations for calibration is also proposed. Bahat and Shakhnarovich (2020) apply semantic preserving transformations such as contrast change, rotation and zoom to augment given inputs and compute confidence using the augmented set of inputs. Jang et al. (2020) introduce a lossy label-invariant transformation for calibration. They define a lossy label-invariant transformation and use it to group inputs and apply group-wise temperature scalings. These approaches do not provide any theoretical bound on the performance as well.

**Calibration with theoretical guarantee.** Kumar et al. (2019) propose a scaling-binning calibrator which combines Platt Scaling and histogram binning, and show the bound on the calibration error. They provide the bound on  $\ell_2$  calibration error and only the debiased estimator for ECE without guarantee, while Hoki provides a bound on  $\ell_1$  calibration error. Park et al. (2020) propose a calibrated prediction method which provides per-prediction confidence bound using Clopper-Pearson interval based on histogram binning. With this method, the inputs in the same bin will have the same confidence interval, while Hoki can assign different confidences to the inputs in the same bin.

## 3. Problem Statement

Let  $\mathcal{X}$  be a feature space,  $\mathcal{Y} = \{1, \dots, C\}$  be a set of labels, and  $\mathcal{D}$  be a distribution over  $\mathcal{X} \times \mathcal{Y}$ . We are given a classifier  $f : \mathcal{X} \rightarrow \mathcal{Y}$  and a corresponding calibrator  $g : \mathcal{X} \rightarrow [0, 1]$  such that, for a given example  $x$ ,  $(f(x), g(x)) = (\hat{y}, \hat{p})$  is the label prediction  $\hat{y}$  with a corresponding confidence  $\hat{p}$ . In what follows, we say that the sets  $\mathcal{P}_1, \dots, \mathcal{P}_J$  form a bin partition of the confidence space,  $[0, 1]$ , if  $\cup_{i=1}^J \mathcal{P}_i = [0, 1]$  and  $\forall i \neq j, \mathcal{P}_i \cap \mathcal{P}_j = \emptyset$ . Furthermore, given a dataset  $Z = \{(x_1, y_1), \dots, (x_N, y_N)\}$ , we say  $g$  induces an index partition  $\mathcal{I}_1, \dots, \mathcal{I}_J$  of  $\{1, \dots, N\}$  such that  $g(x_n) \in \mathcal{P}_j \iff n \in \mathcal{I}_j, \forall (x_n, y_n) \in Z$ .

Before formally stating the problem considered in this work, we define calibration error (CE) and expected calibration error (ECE) (Naeini et al., 2015).

**Definition 1** (Calibration Error (CE)). *For any calibrator  $g$  and confidence partitions  $\mathcal{P}_1, \dots, \mathcal{P}_J$ , the calibration error*

(CE) is defined as

$$CE(g) = \sum_{j=1}^J w_j |e_j|,$$

where

$$e_j := E_{\mathcal{D}} [\mathbb{1}_{\{Y=f(X)\}} - g(X) \mid g(X) \in \mathcal{P}_j]$$

$$w_j := E_{\mathcal{D}} [\mathbb{1}_{\{g(X) \in \mathcal{P}_j\}}].$$

Intuitively, the CE of a classifier-calibrator pair in a given partition is the expected difference between the classifier’s accuracy and the calibrator’s confidence. To get the CE over the entire space, we sum up all the individual partition CEs, weighted by the probability mass of each partition (i.e., the probability of an example falling in that partition).

**Definition 2** (Expected Calibration Error (ECE)). *For any calibrator  $g$ , confidence partitions  $\mathcal{P}_1, \dots, \mathcal{P}_J$ , sampled dataset  $Z \in (\mathcal{X} \times \mathcal{Y})^N$ , and induced index partition  $\{\mathcal{I}_1, \dots, \mathcal{I}_J\}$ , we define the expected calibration error (ECE) as*

$$ECE(g) = \sum_{j=1}^J \hat{w}_j |\hat{e}_j|.$$

where,

$$\hat{e}_j := \sum_{n \in \mathcal{I}_j} \frac{\mathbb{1}_{\{y_n = \hat{y}_n\}} - g(x_n)}{|\mathcal{I}_j|} \quad \text{and} \quad \hat{w}_j := \frac{|\mathcal{I}_j|}{N}.$$

Thus, the ECE is the sampled version of the CE. Note that Definition 2 is equivalent to the standard ECE definition, as used in prior work (Guo et al., 2017). With these definitions in mind, we are now ready to state the problem addressed in this work, namely find a calibrator  $\hat{g}$  that minimizes the ECE over a validation set and provides generalization guarantees in a probably approximately correct (PAC) sense.

**Problem statement 1.** *Let  $\mathcal{G} = \{g : \mathcal{X} \rightarrow [0, 1]\}$  be the set of all calibrators. We aim to find  $\hat{g} \in \mathcal{G}$  that minimizes the expected calibration error,*

$$\hat{g} = \arg \min_{g \in \mathcal{G}} ECE(g)$$

and find a corresponding  $\epsilon$ , for a given  $\delta$ , satisfying a PAC bound on the calibration error

$$P[CE(\hat{g}) \leq \epsilon] \geq 1 - \delta.$$

## 4. Calibration using Transformations

This section provides the intuition and theory of using transformations for the purpose of calibration. The main theoretical contributions of this work are presented in this section and are two fold. First, we introduce a sufficient condition for achieving perfect calibration. Second, we derive a PAC-like claim about the generalization error based on ECE. In the following, we provide high level intuition, followed by our sufficient condition for perfect calibration and generalization error bounds.

### 4.1. High-level Intuition

Suppose that  $f$  and  $g$  form a calibrated classifier-calibrator pair. If we take a correctly classified image of a cat, for example, we would expect that the classification confidence would drop as we apply random transformations to the image (e.g., add noise, zoom out). Conversely, if the confidence does not decrease, we would conclude that  $f$  and  $g$  are not properly calibrated.

More generally, the goal of applying transformations is to group examples in bins of similar confidence. In particular, if a certain set of examples exhibits similar transformation patterns (e.g., label switching, misclassification), then the calibrator should learn to assign such examples a similar confidence value. Of course, this approach would only work for a good choice for transformations – we discuss a number of options in Section 5.

## 4.2. Sufficiency for Perfect Calibration

We now investigate calibrator properties that ensure perfect calibration. Suppose we are given a class of transformation functions  $\mathcal{T} = \{t : \mathcal{X} \rightarrow \mathcal{X}\}$ , e.g., functions that add random noise to an example, and a corresponding probability distribution  $\mathcal{D}_T$  over  $\mathcal{T}$ . Then, for each example  $(x, y)$ , we can apply a number of transformations and observe how many transformations lead to a label switch. Specifically, the following result is key to achieving perfect calibration.

**Theorem 1** (Sufficiency for Perfect Calibration). *Let  $\mathcal{P}_1, \dots, \mathcal{P}_J$  be a confidence bin partition. A calibrator  $g \in \mathcal{G}$  is perfectly calibrated, i.e.,  $CE(g) = 0$ , if it satisfies,  $\forall j \in \{1, \dots, J\}$ ,*

$$E_{\mathcal{D}} [g(X) \mid g(X) \in \mathcal{P}_j] = \alpha_j \gamma_j + \beta_j (1 - \gamma_j)$$

where

$$\begin{aligned} \alpha_j &= E_{\mathcal{D} \times \mathcal{D}_T} [\mathbb{1}_{\{f(X)=Y\}} \mid f(T(X)) = f(X), g(X) \in \mathcal{P}_j] \\ \beta_j &= E_{\mathcal{D} \times \mathcal{D}_T} [\mathbb{1}_{\{f(X)=Y\}} \mid f(T(X)) \neq f(X), g(X) \in \mathcal{P}_j] \\ \gamma_j &= E_{\mathcal{D} \times \mathcal{D}_T} [\mathbb{1}_{\{f(T(X))=f(X)\}} \mid g(X) \in \mathcal{P}_j] \end{aligned}$$

*Proof.* Proof provided in the supplementary material. □

Intuitively, Theorem 1 states that the label switching that we observe (in each bin) due to added transformations must be consistent with the confidence and accuracy in that bin. In particular, the average confidence in the bin must be equal to the weighted sum of accuracies over the two groups of examples: 1) examples whose label is changed by some transformation; 2) examples whose label is not changed due to transformations. The benefit of Theorem 1 is that it leads to a natural implementation by estimating all expectations given a validation set (as discussed in Section 6).

## 4.3. Generalization Bounds on the Calibration Error

While the condition in Theorem 1 ensures perfect calibration in expectation, the best we can do in practice is to achieve those conditions on a sample dataset. Consequently, the question is how well such a calibrator would generalize to unseen data from the same distribution. Leveraging the ECE of a given calibrator, we provide a PAC claim on the generalized calibration error in the following theorem.

**Theorem 2** (Bounded Calibration Error). *Suppose a calibrator  $g$  was calibrated on a dataset  $Z = \{(x_1, y_1), \dots, (x_N, y_N)\}$ . For any  $\delta$ , the CE is bounded, i.e.,*

$$P [CE(g) \leq \epsilon] \geq 1 - \delta,$$

when

$$\epsilon = ECE(g) + \frac{J\sqrt{2}}{\sqrt{N}} \sqrt{2 \ln(2) - \ln(\delta)}$$

*Proof.* Proof provided in the supplementary material. □

Intuitively, Theorem 2 states that to bound the CE, one needs to achieve low ECE on a dataset that is large enough as compared to the number of bins. This result makes sense because one would expect that achieving low CE is harder with more bins since in this case the calibrator needs to perform well on a larger part of the input space (as opposed to performing well on average across the whole input space).

In summary, the theorems developed in this section present a natural approach to the calibration problem. Given a validation set  $Z$ , we first calibrate  $g$  according to the conditions in Theorem 1. Once these conditions are satisfied empirically, we then use Theorem 2 to bound the generalization calibration error of  $g$ . The calibration algorithm is presented in Section 6.

## 5. Transformation Selection

As discussed in Section 4, the choice of transformations greatly affects the benefit of the result presented in Theorem 1. In particular, if a certain transformation results in a label switch for all examples, then it does not provide any useful confidence information. Thus, the most beneficial transformations are those that separate different examples into different partitions, as measured by the proportion of label switches caused by those transformations.

One way of measuring the effect of a given transformation is by estimating  $\alpha$  and  $\beta$  (as defined in Theorem 1) over the entire validation set. Suppose a calibrator  $g$  was calibrated on a validation set  $Z = (x_1, y_1), \dots, (x_N, y_N)$  using a sampled set of transformations  $T = \{t_1, \dots, t_M\}$ , and let  $\mathcal{I}_1, \dots, \mathcal{I}_J$  be the index partition induced by  $g$ . Then, estimates of  $\alpha$  and  $\beta$  can be calculated as

$$\hat{\alpha}_j = \frac{\sum_{n \in \mathcal{I}_j} \sum_{m=1}^M \mathbb{1}_{\{f(x_n)=y_n\}} \mathbb{1}_{\{f(t_m(x_n))=f(x_n)\}}}{\sum_{n \in \mathcal{I}_j} \sum_{m=1}^M \mathbb{1}_{\{f(t_m(x_n))=f(x_n)\}}} \quad (1)$$

$$\hat{\beta}_j = \frac{\sum_{n \in \mathcal{I}_j} \sum_{m=1}^M \mathbb{1}_{\{f(x_n)=y_n\}} \mathbb{1}_{\{f(t_m(x_n)) \neq f(x_n)\}}}{\sum_{n \in \mathcal{I}_j} \sum_{m=1}^M \mathbb{1}_{\{f(t_m(x_n)) \neq f(x_n)\}}} \quad (2)$$

Intuitively,  $\hat{\alpha}$  and  $\hat{\beta}$  both represent the accuracy of the examples; however,  $\hat{\alpha}$  is determined over the set of examples and transformations where the network does not change prediction, while  $\hat{\beta}$  is determined over the set of examples and transformations where the network does change prediction. Thus, if a transformation results in a large difference between  $\hat{\alpha}$  and  $\hat{\beta}$ , that means this transformation is correlated with the classifier’s sensitivity to input perturbations and hence with the confidence in the classifier’s correctness. Therefore, we aim to identify transformations that maximize the difference between  $\hat{\alpha}$  and  $\hat{\beta}$  on the validation set.

The first consideration when selecting a transformation is whether to apply it to the input  $x$  or to some internal classifier representation, *e.g.*, the logits in last layer of a neural network. The benefits of applying input transformations are that they are independent of the classifier and can be chosen based on physical characteristics (*e.g.*, a small rotation should not affect an image’s class). Applying transformations to the logits is also appealing due to the reduced dimensionality: this results in improved scalability and makes it easier to find useful transformations.

The last consideration when choosing the transformations is what family to select them from. Input transformations offer a wide range of possibilities, especially in the case of images, *e.g.*, rotation, translation, zoom out. On the other hand, logit transformations do not necessarily have a physical interpretation, so a more natural choice is to add noise selected from a known probability distribution, *e.g.*, Gaussian or uniform.

In this paper, we explore the space of uniform noise, as applied to the neural network’s logits.<sup>1</sup> To choose the noise range, we search over the space  $[-20, 20]$  for both the minimum and maximum noise and select the pair that results in the largest difference between  $\hat{\alpha}$  and  $\hat{\beta}$  on the validation set.

Table 1 shows the selected transformation parameters and corresponding values for  $\hat{\alpha}$  and  $\hat{\beta}$ , as computed over the different datasets and models used in our experiments (please refer to Section 7 for a full description of the datasets). As shown in the table, the absolute difference between  $\hat{\alpha}$  and  $\hat{\beta}$  varies between 0.2275 and 0.5695, which illustrates the challenge of finding an appropriate transformation.

<sup>1</sup>While we tried a number of different logit and input transformations, we found that adding uniform noise consistently resulted in the best empirical performance.



Table 1. Selected transformation parameters over the different datasets and models.

DATASET	MODEL	PARAMETERS	$\hat{\alpha}$	$\hat{\beta}$	$ \hat{\alpha} - \hat{\beta} $
MNIST	LENET 5	(16, 17)	0.9892	0.4197	0.5695
CIFAR10	DENSENET 40	(13, 14)	0.9219	0.4166	0.5053
	LENET 5	(-8, -7)	0.7453	0.3830	0.3623
	RESNET 110	(1, 2)	0.9435	0.4700	0.4735
	RESNET 110 SD	(-15, -14)	0.9070	0.4586	0.4484
	WRN 28-10	(10, 11)	0.9620	0.4685	0.4935
CIFAR100	DENSENET 40	(-20, -19)	0.7016	0.2967	0.4049
	LENET 5	(-5, 1)	0.4817	0.2542	0.2275
	RESNET 110	(-13, -12)	0.7216	0.3255	0.3961
	RESNET 110 SD	(-13, -12)	0.7223	0.3159	0.4064
	WRN 28-10	(10, 11)	0.8103	0.3064	0.5039
IMAGENET	DENSENET 161	(-5, -4)	0.7855	0.3281	0.4574
	MOBILENET V2	(-17, -16)	0.7408	0.3089	0.4319
	RESNET 152	(8, 9)	0.7961	0.3371	0.4590
	WRN 101-2	(12, 13)	0.8017	0.3423	0.4594

## 6. Implementation

Based on the theory described in Section 4, we propose Hoki, an iterative algorithm for confidence calibration. Hoki operates differently during design time and runtime. During design time, Hoki samples random transformations and learns the corresponding  $\hat{\alpha}$  and  $\hat{\beta}$  parameters used to partition the data. These parameters are then used at runtime, on test data, to calibrate the confidence given new examples.

### 6.1. Design Time Algorithm

The design time algorithm is described in Algorithm 1. The high-level idea of the algorithm is to achieve the sufficient condition outlined in Theorem 1 on the validation set. In particular, we first sample transformations  $\{t_1, \dots, t_M\}$  from  $\mathcal{T}$  and observe the corresponding predictions  $\tilde{y}_{n,m}$ . Based on  $\tilde{y}_{n,m}$ , we compute the fraction of transformed examples that have the same label as the original image,  $\gamma_n$ . We emphasize that, as a special case of Theorem 1,  $\gamma_n$  is computed separately for each example, as opposed to averaged over the entire partition. This modification ensures that the data is spread across multiple partitions, while still satisfying the sufficient condition for perfect calibration.

After the initialization step, Hoki recursively estimates the parameters  $\alpha_j$  and  $\beta_j$  and computes the calibrated confidence using those two values based on Theorem 1. Since the original partitioning may change after reestimating the parameters, we repeat this process until there is no change in the data partitioning (or a maximum number of iterations is reached). Note that for the corner case where the transformations result in empty sets (i.e., either all labels change or all remain the same), we set  $\hat{\alpha}_j^k, \hat{\beta}_j^k$  to the bin accuracy. Ultimately, at design time, Hoki returns the set of calibration pairs for all partitions for all iterations learned in the design time algorithm as a set  $\mathcal{H}$ , the set of transformations  $\hat{\mathcal{T}}$ , and the validation data accuracy,  $p$ .

### 6.2. Runtime Algorithm

The runtime algorithm is described in Algorithm 2. Once the parameters for each step,  $\hat{\alpha}_j^k$  and  $\hat{\beta}_j^k$ , are learnt in Algorithm 1, Hoki can calibrate the confidence for a new input  $x$  using the calibration parameter pairs in  $\mathcal{H}$ . Hoki first observes the original prediction  $f(x)$  and the transformed data prediction  $f(t_m(x))$  for all transformations  $\{t_1, t_2, \dots, t_M\}$ . Hoki computes  $\gamma$  based on these values and iteratively updates the confidence according to the calibration parameters learned in Algorithm 1.

### 6.3. Memory Complexity

In terms of memory complexity, Hoki estimates the validation data accuracy and two parameters for each bin  $j$ , namely  $\hat{\alpha}_j$  and  $\hat{\beta}_j$ . Since we perform the estimation iteratively  $K^*$  times (where  $K^*$  is the number of iterations required for Algorithm 1 to terminate), the total number of estimated parameters is  $2 \times J \times K^* + 1$  parameters. Considering that the standard number of bins in the literature is  $J = 15$  (Guo et al., 2017; Nixon et al., 2019) and the algorithm finishes with  $K^* < 5$  on 13 of 15 benchmarks in this paper, we conclude that Hoki requires little memory for its storage.

**Algorithm 1** Design Time Algorithm

**Input:** validation set  $Z = (x_1, y_1), \dots, (x_N, y_N)$ , transformation set  $\mathcal{T}$ , number of transformations  $M$ , classifier  $f$ , confidence space partition  $\mathcal{P}_1, \dots, \mathcal{P}_J$ , maximum number of iterations  $K$

Sample transformations  $\hat{\mathcal{T}} = \{t_1, \dots, t_M\}$  from  $\mathcal{T}$

$$\hat{p} = \frac{1}{N} \sum_{n=1}^N \mathbb{1}_{\{y_n=f(x_n)\}}$$

**for**  $n = 1$  **to**  $N$  **do**

$$\hat{\gamma}_n = \frac{1}{M} \sum_{m=1}^M \mathbb{1}_{\{f(t_m(x_n))=f(x_n)\}}$$

$$p_n = \hat{p}$$

**end for**

**for**  $k = 1$  **to**  $K$  **do**

Compute sets  $\mathcal{I}_1^k, \dots, \mathcal{I}_J^k$  s. t.  $n \in \mathcal{I}_j^k \iff p_n \in \mathcal{P}_j$

**if**  $k > 1 \wedge \mathcal{I}_1^k = \mathcal{I}_1^{k-1} \wedge \dots \wedge \mathcal{I}_J^k = \mathcal{I}_J^{k-1}$  **then**

**break**

**end if**

**for**  $j = 1$  **to**  $J$  **do**

$$c = \sum_{n \in \mathcal{I}_j^k} \sum_{m=1}^M \mathbb{1}_{\{f(x_n)=f(t_m(x_n))\}}$$

**if**  $c = 0 \vee c = M|\mathcal{I}_j^k|$  **then**

$$\hat{\alpha}_j^k = \hat{\beta}_j^k = \frac{1}{|\mathcal{I}_j^k|} \sum_{n \in \mathcal{I}_j^k} \mathbb{1}_{\{y_n=f(x_n)\}}$$

**else**

Compute  $\hat{\alpha}_j^k$  according to Equation (1), using  $\mathcal{I}_j^k$

Compute  $\hat{\beta}_j^k$  according to Equation (2), using  $\mathcal{I}_j^k$

**end if**

$$p_n = \left( \hat{\alpha}_j^k - \hat{\beta}_j^k \right) \hat{\gamma}_n + \hat{\beta}_j^k, \forall n \in \mathcal{I}_j^k$$

**end for**

$$K^* = k$$

**end for**

$$\mathcal{H} = \{(\hat{\alpha}_j^k, \hat{\beta}_j^k) \mid 1 \leq j \leq J, 1 \leq k \leq K^*\}$$

return  $\mathcal{H}, \hat{p}, \hat{\mathcal{T}}$

## 7. Experiments

We compare Hoki with state-of-the-art calibration algorithms using several standard datasets and models. For each model and dataset, we compute the ECE for the uncalibrated model and the calibrated confidence by the algorithms. The experimental setup, baseline algorithms and the evaluation metrics are explained in the following subsections.

### 7.1. Experimental Setup

This subsection provides the details about the datasets, models, baseline algorithms, and the evaluation metrics.

**Datasets and Models.** We perform experiments on the following four different datasets.

- MNIST (LeCun et al., 1998). A handwritten dataset of  $28 \times 28$  images. 60,000 training data and 10,000 test data. We extract 10,000 images from the training data as validation data.
- CIFAR 10/100 (Krizhevsky et al., 2009). A 10/100-class dataset of  $32 \times 32$  color images. 50,000 training data and 10,000 test data. We extract 5,000 images from the training data as validation data.
- ImageNet (Deng et al., 2009). A 1,000-class dataset consisting of  $224 \times 224$  color images. 1.3M training data and 50,000 validation data. We divide the validation set into two sets of 25,000 data, one for a validation set and one for a test set.

We use the following models for each dataset. For MNIST, we use one model, LeNet5 (LeCun et al., 1998). For CIFAR



**Algorithm 2** Runtime Algorithm

**Input:** test sample  $x \in \mathcal{X}$ , original classifier  $f$ , outputs of Algorithm 1:  $\mathcal{H}, \hat{p}, \hat{\mathcal{T}}$ .

$$\gamma = \frac{1}{M} \sum_{m=1}^M \mathbb{1}_{\{f(x)=f(t_m(x))\}}, t_m \in \hat{\mathcal{T}}$$

$$p = \hat{p}$$

**for**  $k = 1$  **to**  $\frac{|\mathcal{H}|}{J}$  **do**

Identify partition index  $j'$  for  $x$  such that  $p \in \mathcal{P}_{j'}$

Identify calibration parameters  $(\hat{\alpha}_{j'}^k, \hat{\beta}_{j'}^k) \in \mathcal{H}$

$$p = (\alpha_{j'}^k - \beta_{j'}^k) \gamma + \beta_{j'}^k$$

**end for**

return  $p$

10/100, we use five different models, DenseNet 40 (Huang et al., 2017), LeNet5 (LeCun et al., 1998), ResNet110 (He et al., 2016), ResNet110 SD (Huang et al., 2016), and WRN-28-10 (Zagoruyko & Komodakis, 2016). For ImageNet, we use four models, DenseNet161 (Huang et al., 2017), MobileNetV2 (Sandler et al., 2018), ResNet152 (He et al., 2016), and WRN-101-2 (Zagoruyko & Komodakis, 2016).

We implement LeNet5, ResNet110 SD, and obtain code for DenseNet40<sup>2</sup>, ResNet110<sup>3</sup> and WRN 28-10<sup>3</sup> from the corresponding github repositories. We also obtained the pre-trained model for all models on ImageNet from PyTorch.<sup>4</sup>

**Baselines.** We compare Hoki with several state-of-the-art calibration algorithms, namely temperature scaling, vector scaling (Guo et al., 2017), Dir-ODIR, MS-ODIR (Kull et al., 2019) and ReCal (Jang et al., 2020). They calibrate confidence by learning a mapping function for uncalibrated logits or confidences. We obtain other calibration algorithms from their papers except for temperature scaling and vector scaling which we obtain from Kull et al. (2019). For ReCal, the authors provide three different setups for their algorithm, and we choose ('zoom-out', 0.1, 0.9, 20) because it shows the best results on ImageNet.

**Evaluation Metric.** As described in Problem Statement 1, we evaluate all algorithms based on ECE, as defined in Definition 2. Additionally, we calculate the learning time during design time to investigate each algorithm's practical utility. If a calibration algorithm is too slow on real datasets, it may not be appropriate to use the algorithm in practice.

## 7.2. Results

The experimental results have two parts. The first part is a comparison on calibration performance in terms of ECE, and the second part is an analysis on time efficiency during design time.

### 7.2.1. ECE RESULTS

Table 2 displays ECE values for each calibration algorithm, along with each model's validation set and test set accuracy. As discussed in Section 5, Hoki uses the transformations shown in Table 1.

As shown in Table 2, Hoki achieves the lowest ECE on 10 out of 15 benchmarks. The benefit of using transformations is especially pronounced in the large-dimensional ImageNet dataset where Hoki achieves the lowest ECE on all models and is on average an order of magnitude better than the other methods.

Interestingly, the ECE produced by Hoki closely tracks the difference between the validation and test set accuracy. In some sense, one cannot hope to do better than this difference as it reflects the variance within each dataset. Thus, the benchmarks where Hoki does not achieve the best performance are settings with large differences in generalization accuracy. For example, in the case of ResNet110 on CIFAR10 and CIFAR100, the gaps are 1.02 and 1.08 percentage points, respectively.

Another reason for our strong performance on ImageNet is the dataset size (there are 25,000 images in the ImageNet validation set compared to 10,000 images in MNIST and 5,000 images in CIFAR10/100). A larger validation set means that each partition is likely to have more samples, which in turn results in more accurate estimation of  $\alpha$ ,  $\beta$ , and  $\gamma$ . Furthermore, as shown in Theorem 2, Hoki achieves better generalization error bounds as the size of the dataset increases.

<sup>2</sup><https://github.com/andreasveit/densenet-pytorch>

<sup>3</sup><https://github.com/bearpaw/pytorch-classification>

<sup>4</sup><https://pytorch.org/docs/stable/torchvision/models.html>

**Confidence Calibration with Bounded Error Using Transformations**

Table 2. ECE for the different calibration algorithms on different datasets and models. The number with the bold face and the underline denote the best and the second best result, respectively.

DATASET	MODEL	VAL ACC. (%)	TEST ACC. (%)	UNCAL.	TEMPS	VECS	MS-ODIR	DIR-ODIR	RECAL	HOKI
MNIST	LeNET5	98.85	98.81	0.007639	0.001834	<b>0.001459</b>	0.002388	0.002236	0.002149	<u>0.001755</u>
CIFAR10	DENSENET 40	91.92	91.75	0.052026	0.007037	<u>0.004438</u>	0.005161	0.003943	0.010143	<b>0.002485</b>
	LeNET5	72.00	72.77	0.018170	0.011963	<b>0.009174</b>	0.014147	<u>0.010525</u>	0.011785	0.017294
	RESNET110	94.12	93.10	0.045646	<u>0.008770</u>	0.009442	0.008829	<b>0.008366</b>	0.008986	0.012247
	RESNET110 SD	90.28	90.38	0.053770	0.011407	<u>0.008552</u>	0.010187	0.009369	0.011973	<b>0.004848</b>
	WRN 28-10	96.06	95.94	0.025076	0.009709	<u>0.009564</u>	0.009175	0.009429	<u>0.009092</u>	<b>0.002483</b>
CIFAR100	DENSENET 40	68.82	68.16	0.172838	0.015435	0.026634	0.029628	0.018949	<u>0.015398</u>	<b>0.008907</b>
	LeNET5	37.82	37.66	<u>0.009991</u>	0.021064	0.015524	0.013149	0.014172	0.019196	<b>0.009859</b>
	RESNET 110	70.60	69.52	0.142223	<b>0.009101</b>	0.029982	0.034519	0.023109	<u>0.012142</u>	0.014866
	RESNET 110 SD	70.62	70.10	0.122932	<b>0.009310</b>	0.035832	0.035478	0.020747	<u>0.009987</u>	0.011003
	WRN 28-10	79.62	79.90	0.053396	0.043703	0.045178	0.035509	<u>0.034604</u>	0.037270	<b>0.009975</b>
IMAGENET	DENSENET 161	76.83	77.45	0.056384	0.019873	0.023286	0.036785	0.047707	<u>0.013348</u>	<b>0.002824</b>
	MOBILENET V2	71.69	72.01	0.027421	0.016379	0.015287	0.021198	0.026880	<u>0.015253</u>	<b>0.002487</b>
	RESNET 152	77.93	78.69	0.049142	0.020069	0.020672	0.034736	0.039748	<u>0.013869</u>	<b>0.004296</b>
	WRN 101-2	78.67	79.15	0.052429	0.030690	0.032993	0.041626	0.027887	<u>0.025785</u>	<b>0.005335</b>

Table 3. Learning time (sec). The number with the bold face and the underline are the best and the second best result, respectively.

DATASET	MODEL	TEMPS	VECS	MS-ODIR	DIR-ODIR	RECAL	HOKI
MNIST	LeNET5	<b>0.16</b>	43.31	112.04	207.88	57.67	<u>0.64</u>
CIFAR10	DENSENET40	<b>0.08</b>	31.33	222.93	92.34	84.04	<u>0.33</u>
	LeNET5	<b>0.05</b>	11.86	79.62	74.33	110.79	<u>0.30</u>
	RESNET110	<b>0.07</b>	27.17	193.04	87.73	38.85	<u>0.32</u>
	RESNET110 SD	<b>0.07</b>	21.39	189.27	93.17	58.74	<u>0.26</u>
	WRN 28-10	<b>0.05</b>	22.71	123.46	92.80	49.62	<u>0.47</u>
CIFAR100	DENSENET40	<b>0.51</b>	23.17	1211.68	626.00	136.23	<u>1.18</u>
	LeNET5	<b>0.42</b>	24.17	459.59	236.87	97.77	<u>1.19</u>
	RESNET110	<b>0.30</b>	25.49	1459.71	510.12	97.29	<u>1.02</u>
	RESNET110 SD	<b>0.24</b>	25.51	1696.10	495.23	604.12	<u>1.06</u>
	WRN 28-10	<b>0.30</b>	26.71	1110.11	611.52	125.84	<u>1.10</u>
IMAGENET	DENSENET161	<b>18.79</b>	179.61	13901.38	6891.19	50730.17	<u>34.61</u>
	MOBILENET V2	<b>18.74</b>	423.48	3899.07	12695.64	3139.60	<u>39.87</u>
	RESNET152	<b>18.79</b>	169.72	12401.58	5402.85	71254.34	<u>33.70</u>
	WRN 101-2	<b>18.73</b>	182.39	16989.40	11378.40	31545.77	<u>33.94</u>

7.2.2. ANALYSIS ON TIME EFFICIENCY

Table 3 displays the learning time of each calibration algorithm during design time. Hoki is always the second fastest algorithm next to temperature scaling during design time. The main reason for the proposed method’s good scalability is that we apply transformations to the logits – thus, we avoid the need to perform the input transformations that are needed in ReCal, for example. Furthermore, Hoki is comparable to temperature scaling, which is fairly simple approaches in the sense that it only needs to learn one parameter.

In summary, Hoki not only achieves the lowest ECE on almost all benchmarks but is also the fast algorithm.

## 8. Conclusion

This work proposed a confidence calibration algorithm with a theoretical bound on the ECE. Our approach is based on the intuition that we can partition examples based on the neural network’s sensitivity to transformations. In particular, if a set of examples result in a similar number of label switches upon being transformed, then the calibrator should assign similar confidences to such examples. Based on this intuition, we provide a sufficient condition for perfect calibration in terms of ECE, and also provide conditions under which the calibration error on new examples is bounded. Finally, we provide an extensive experimental comparison and demonstrate that Hoki outperforms state-of-the-art approaches in multiple datasets and models, and the benefits are especially pronounced on the challenging ImageNet.

For future work, we plan to explore the benefits of combining different transformations, particularly a mix of input and logit transformations. If those transformations are chosen carefully in order to identify input sensitivity, we expect that more accurate calibration is possible. In another avenue of future work, we aim to combine Hoki with other calibration techniques as well, *e.g.*, by initializing the confidence estimation using confidences obtained by other algorithms.

## References

- Arcadu, F., Benmansour, F., Maunz, A., Willis, J., Haskova, Z., and Prunotto, M. Deep learning algorithm predicts diabetic retinopathy progression in individual patients. *NPJ digital medicine*, 2(1):1–9, 2019.
- Bahat, Y. and Shakhnarovich, G. Classification confidence estimation with test-time data-augmentation. *arXiv preprint arXiv:2006.16705*, 2020.
- Bochkovskiy, A., Wang, C.-Y., and Liao, H.-Y. M. Yolov4: Optimal speed and accuracy of object detection. *arXiv preprint arXiv:2004.10934*, 2020.
- Deng, J., Dong, W., Socher, R., Li, L.-J., Li, K., and Fei-Fei, L. Imagenet: A large-scale hierarchical image database. In *2009 IEEE conference on computer vision and pattern recognition*, pp. 248–255. Ieee, 2009.
- Guo, C., Pleiss, G., Sun, Y., and Weinberger, K. Q. On calibration of modern neural networks. *arXiv preprint arXiv:1706.04599*, 2017.
- Gupta, K., Rahimi, A., Ajanthan, T., Mensink, T., Sminchisescu, C., and Hartley, R. Calibration of neural networks using splines. *arXiv preprint arXiv:2006.12800*, 2020.
- He, K., Zhang, X., Ren, S., and Sun, J. Deep residual learning for image recognition. In *Proceedings of the IEEE conference on computer vision and pattern recognition*, pp. 770–778, 2016.
- Huang, G., Sun, Y., Liu, Z., Sedra, D., and Weinberger, K. Q. Deep networks with stochastic depth. In *European conference on computer vision*, pp. 646–661. Springer, 2016.
- Huang, G., Liu, Z., Van Der Maaten, L., and Weinberger, K. Q. Densely connected convolutional networks. In *Proceedings of the IEEE conference on computer vision and pattern recognition*, pp. 4700–4708, 2017.
- Jang, S., Lee, I., and Weimer, J. Improving classifier confidence using lossy label-invariant transformations. *arXiv preprint arXiv:2011.04182*, 2020.
- Krizhevsky, A., Hinton, G., et al. Learning multiple layers of features from tiny images. 2009.
- Kull, M., Nieto, M. P., Kängsepp, M., Silva Filho, T., Song, H., and Flach, P. Beyond temperature scaling: Obtaining well-calibrated multi-class probabilities with dirichlet calibration. In *Advances in Neural Information Processing Systems*, pp. 12295–12305, 2019.
- Kumar, A., Sarawagi, S., and Jain, U. Trainable calibration measures for neural networks from kernel mean embeddings. In *International Conference on Machine Learning*, pp. 2805–2814, 2018.
- Kumar, A., Liang, P., and Ma, T. Verified uncertainty calibration. *arXiv preprint arXiv:1909.10155*, 2019.
- LeCun, Y., Bottou, L., Bengio, Y., and Haffner, P. Gradient-based learning applied to document recognition. *Proceedings of the IEEE*, 86(11):2278–2324, 1998.

- Li, C., Ma, X., Jiang, B., Li, X., Zhang, X., Liu, X., Cao, Y., Kannan, A., and Zhu, Z. Deep speaker: an end-to-end neural speaker embedding system. *arXiv preprint arXiv:1705.02304*, 650, 2017.
- Naeni, M. P., Cooper, G. F., and Hauskrecht, M. Obtaining well calibrated probabilities using bayesian binning. In *Proceedings of the... AAAI Conference on Artificial Intelligence. AAAI Conference on Artificial Intelligence*, volume 2015, pp. 2901. NIH Public Access, 2015.
- Nixon, J., Dusenberry, M. W., Zhang, L., Jerfel, G., and Tran, D. Measuring calibration in deep learning. In *CVPR Workshops*, volume 2, 2019.
- Park, S., Li, S., Bastani, O., and Lee, I. Pac confidence predictions for deep neural network classifiers. *arXiv preprint arXiv:2011.00716*, 2020.
- Patel, K., Beluch, W., Yang, B., Pfeiffer, M., and Zhang, D. Multi-class uncertainty calibration via mutual information maximization-based binning. *arXiv preprint arXiv:2006.13092*, 2020.
- Platt, J. et al. Probabilistic outputs for support vector machines and comparisons to regularized likelihood methods. *Advances in large margin classifiers*, 10(3):61–74, 1999.
- Rahimi, A., Shaban, A., Cheng, C.-A., Hartley, R., and Boots, B. Intra order-preserving functions for calibration of multi-class neural networks. *Advances in Neural Information Processing Systems*, 33, 2020.
- Redmon, J. and Farhadi, A. Yolov3: An incremental improvement. *arXiv preprint arXiv:1804.02767*, 2018.
- Ronneberger, O., Fischer, P., and Brox, T. U-net: Convolutional networks for biomedical image segmentation. In *International Conference on Medical image computing and computer-assisted intervention*, pp. 234–241. Springer, 2015.
- Sandler, M., Howard, A., Zhu, M., Zhmoginov, A., and Chen, L.-C. Mobilenetv2: Inverted residuals and linear bottlenecks. In *Proceedings of the IEEE conference on computer vision and pattern recognition*, pp. 4510–4520, 2018.
- Seo, S., Seo, P. H., and Han, B. Learning for single-shot confidence calibration in deep neural networks through stochastic inferences. In *Proceedings of the IEEE Conference on Computer Vision and Pattern Recognition*, pp. 9030–9038, 2019.
- Tan, M. and Le, Q. Efficientnet: Rethinking model scaling for convolutional neural networks. In *International Conference on Machine Learning*, pp. 6105–6114. PMLR, 2019.
- Tran, G.-L., Bonilla, E. V., Cunningham, J., Michiardi, P., and Filippone, M. Calibrating deep convolutional gaussian processes. In *The 22nd International Conference on Artificial Intelligence and Statistics*, pp. 1554–1563, 2019.
- Wenger, J., Kjellström, H., and Triebel, R. Non-parametric calibration for classification. In *International Conference on Artificial Intelligence and Statistics*, pp. 178–190. PMLR, 2020.
- Zagoruyko, S. and Komodakis, N. Wide residual networks. *arXiv preprint arXiv:1605.07146*, 2016.

---

## Confidence Calibration with Bounded Error Using Transformation: Supplementary Material

---

### A. Proof of Theorem 1

We begin by observing for any  $g$  and  $\mathcal{P}_j \in \{\mathcal{P}_1, \dots, \mathcal{P}_J\}$ , the law of total probability states

$$\begin{aligned}
 E [\mathbb{1}_{\{Y=f(X)\}} \mid g(X) \in \mathcal{P}_j] &= \\
 &= E [\mathbb{1}_{\{Y=f(X)\}} \mid f(T(X)) = f(X), g(X) \in \mathcal{P}_j] E [\mathbb{1}_{\{f(T(X))=f(X)\}} \mid g(X) \in \mathcal{P}_j] \\
 &\quad + E [\mathbb{1}_{\{Y=f(X)\}} \mid f(T(X)) \neq f(X), g(X) \in \mathcal{P}_j] E [\mathbb{1}_{\{f(T(X))\neq f(X)\}} \mid g(X) \in \mathcal{P}_j] \\
 &= \alpha_j \gamma_j + \beta_j E [\mathbb{1}_{\{f(T(X))\neq f(X)\}} \mid g(X) \in \mathcal{P}_j] \\
 &= \alpha_j \gamma_j + \beta_j (1 - \gamma_j)
 \end{aligned}$$

Next we observe that the expected calibration error (ECE) over a  $J$ -binning of confidence for and  $g \in \mathcal{G}$  can be written as

$$CE(g) = \sum_{j=1}^J w_j |e_j| = \sum_{j=1}^J w_j \left| \alpha_j \gamma_j + \beta_j (1 - \gamma_j) - E[g(X) \mid g(X) \in \mathcal{P}_j] \right|$$

Thus, we conclude that it is sufficient to claim that  $g \in \mathcal{G}$  minimizes the calibration error – *i.e.*,  $CE(g) = 0$  – if it satisfies

$$\forall j \in \{1, \dots, J\}, E[g(X) \mid g(X) \in \mathcal{P}_j] = \alpha_j \gamma_j + \beta_j (1 - \gamma_j)$$

## B. Proof of Theorem 2

$$\begin{aligned}
 P[CE(\hat{g}) \geq \epsilon] &= \\
 &= P \left[ \sum_{j=1}^J |e_j| w_j \geq \epsilon \right] \\
 &= P \left[ \sum_{j=1}^J |e_j| (w_j - \hat{w}_j + \hat{w}_j) \geq \epsilon \right] \\
 &\leq P \left[ \sum_{j=1}^J |e_j| |w_j - \hat{w}_j| + |e_j| \hat{w}_j \geq \epsilon \right] \\
 &\leq P \left[ \sum_{j=1}^J |w_j - \hat{w}_j| + |e_j| \hat{w}_j \geq \epsilon \right] \\
 &\leq P \left[ \sum_{j=1}^J |w_j - \hat{w}_j| + |e_j - \hat{e}_j| \hat{w}_j + |\hat{e}_j| \hat{w}_j \geq \epsilon \right] \\
 &= P \left[ \sum_{j=1}^J |w_j - \hat{w}_j| + |e_j - \hat{e}_j| \hat{w}_j \geq \epsilon - ECE(\hat{g}) \right] \\
 &\leq \max_j P \left[ |w_j - \hat{w}_j| + |e_j - \hat{e}_j| \hat{w}_j \geq \frac{\epsilon - ECE(\hat{g})}{J} \right] \\
 &\leq \max_j P \left[ |w_j - \hat{w}_j| \geq \frac{\epsilon - ECE(\hat{g})}{2J} \right] + P \left[ |e_j - \hat{e}_j| \geq \frac{\epsilon - ECE(\hat{g})}{2J\hat{w}_j} \right] \\
 &\leq \max_j 2 \exp \left\{ -2N \left( \frac{\epsilon - ECE(\hat{g})}{2J} \right)^2 \right\} + 2 \exp \left\{ -2N\hat{w}_j \left( \frac{\epsilon - ECE(\hat{g})}{2J\hat{w}_j} \right)^2 \right\} \\
 &= \max_j 2 \exp \left\{ -2N \left( \frac{\epsilon - ECE(\hat{g})}{2J} \right)^2 \right\} + 2 \exp \left\{ -2N \frac{1}{\hat{w}_j} \left( \frac{\epsilon - ECE(\hat{g})}{2J} \right)^2 \right\} \\
 &\leq 2 \exp \left\{ -2N \left( \frac{\epsilon - ECE(\hat{g})}{2J} \right)^2 \right\} + 2 \exp \left\{ -2N \left( \frac{\epsilon - ECE(\hat{g})}{2J} \right)^2 \right\} \\
 &= 4 \exp \left\{ -\frac{N(\epsilon - ECE(\hat{g}))^2}{2J^2} \right\}
 \end{aligned}$$

We complete the proof by observing

$$4 \exp \left\{ -\frac{N(\epsilon - ECE(\hat{g}))^2}{2J^2} \right\} \leq \delta \iff \epsilon \geq ECE(\hat{g}) + \frac{J\sqrt{2}}{\sqrt{N}} \sqrt{(2 \ln(2) - \ln(\delta))}$$

## C. Additional Experiments

In this section, we present additional experimental results. We show the ECE values by Hoki with different number of bins, and with the different initialization.

### C.1. Number of bins

In addition to the general setting of 15 bins ( $J = 15$ ), we use 30 bins ( $J = 30$ ) as well. As shown in Table 4, for all datasets and models except ResNet152 on ImageNet, Hoki with 15 bins outperforms Hoki with 30 bins. Even for the exception, the



difference is small compared to other cases. We can expect this result by Theorem 1. As mentioned in Section 4, Theorem 1 shows that it is hard to obtain low ECE with more bins.

Table 4. ECE by different number of bins: 15 vs. 30

DATASET	MODEL	$J = 15$	$J = 30$
MNIST	LENET 5	<b>0.001755</b>	0.002015
CIFAR10	DENSENET 40	<b>0.002485</b>	0.006053
	LENET 5	<b>0.017294</b>	0.017720
	RESNET 110	<b>0.012247</b>	0.013939
	RESNET 110 SD	<b>0.004848</b>	0.005604
	WRN 28-10	<b>0.002483</b>	0.004758
CIFAR100	DENSENET 40	<b>0.008907</b>	0.011074
	LENET 5	<b>0.009859</b>	0.011592
	RESNET 110	<b>0.014866</b>	0.015647
	RESNET 110 SD	<b>0.011003</b>	0.013410
	WRN 28-10	<b>0.009975</b>	0.010189
IMAGENET	DENSENET 161	<b>0.002824</b>	0.003376
	MOBILENET V2	<b>0.002487</b>	0.003185
	RESNET 152	0.004296	<b>0.004226</b>
	WRN 101-2	<b>0.005335</b>	0.005457

### C.2. Initialization with Original Uncalibrated Confidence

We perform an experiment to investigate the effect of the different initialization. In Algorithm 1 and 2, we initialize the confidence with the validation set accuracy. We can also use the original uncalibrated confidence from a classifier as the initial value, and we compare ECE values with those two different initialization. Table 5 shows that the initialization with the validation set accuracy is always better than the initialization with original uncalibrated confidence. We think that the transformation selection method results in this performance difference. As described in Section 5, we decide transformation based on the difference  $\hat{\alpha}$  and  $\hat{\beta}$  after putting all examples in one bin. However, with the original uncalibrated confidence initialization, the examples are spread over different bins, and we need to find a different method for searching appropriate transformations.

Table 5. ECE by different initialization

DATASET	MODEL	VAL ACCURACY	ORIGINAL
MNIST	LENET 5	<b>0.001755</b>	0.003743
CIFAR10	DENSENET 40	<b>0.002485</b>	0.017593
	LENET 5	<b>0.017294</b>	0.022682
	RESNET 110	<b>0.012247</b>	0.017556
	RESNET 110 SD	<b>0.004848</b>	0.026936
	WRN 28-10	<b>0.002483</b>	0.013858
CIFAR100	DENSENET 40	<b>0.008907</b>	0.096884
	LENET 5	<b>0.009859</b>	0.018897
	RESNET 110	<b>0.014866</b>	0.026153
	RESNET 110 SD	<b>0.011003</b>	0.041084
	WRN 28-10	<b>0.009975</b>	0.027175
IMAGENET	DENSENET 161	<b>0.002824</b>	0.044149
	MOBILENET V2	<b>0.002487</b>	0.029067
	RESNET 152	<b>0.004296</b>	0.026629
	WRN 101-2	<b>0.005335</b>	0.036469